

## Article

# Liquid-Phase Selective Hydrogenation of Furfural to Furfuryl Alcohol over Ferromagnetic Element (Fe, Co, Ni, Nd)-Promoted Pt Catalysts Supported on Activated Carbon

Sureeporn Saknaphawuth <sup>1</sup>, Patcharaporn Weerachawanasak <sup>2</sup>, Laemthong Chuenchom <sup>3</sup> , Piyasan Praserttham <sup>1</sup> and Joongjai Panpranot <sup>1,4,5,\*</sup> 

<sup>1</sup> Center of Excellence on Catalysis and Catalytic Reaction Engineering, Department of Chemical Engineering, Faculty of Engineering, Chulalongkorn University, Bangkok 10330, Thailand; champagne\_jeab@hotmail.com (S.S.); piyasan.p@chula.ac.th (P.P.)

<sup>2</sup> Department of Chemistry, Faculty of Science, King Mongkut's Institute of Technology Ladkrabang, Bangkok 10520, Thailand; patcharaporn.we@kmitl.ac.th

<sup>3</sup> Department of Chemistry, Faculty of Science, Prince of Songkla University, Songkhla 90112, Thailand; laemthong.c@psu.ac.th

<sup>4</sup> Bio-Circular-Green-Economy Technology & Engineering Center, BCGeTEC, Department of Chemical Engineering, Faculty of Engineering, Chulalongkorn University, Bangkok 10330, Thailand

<sup>5</sup> Department of Chemical & Petroleum Engineering, Faculty of Engineering, Technology and Built Environment, UCSI University, Kuala Lumpur 56000, Malaysia

\* Correspondence: joongjai.p@chula.ac.th; Tel.: +66-2218-6869; Fax: +66-2218-6877



**Citation:** Saknaphawuth, S.; Weerachawanasak, P.; Chuenchom, L.; Praserttham, P.; Panpranot, J. Liquid-Phase Selective Hydrogenation of Furfural to Furfuryl Alcohol over Ferromagnetic Element (Fe, Co, Ni, Nd)-Promoted Pt Catalysts Supported on Activated Carbon. *Catalysts* **2022**, *12*, 393. <https://doi.org/10.3390/catal12040393>

Academic Editor: Weijian Diao

Received: 9 February 2022

Accepted: 29 March 2022

Published: 31 March 2022

**Publisher's Note:** MDPI stays neutral with regard to jurisdictional claims in published maps and institutional affiliations.



**Copyright:** © 2022 by the authors. Licensee MDPI, Basel, Switzerland. This article is an open access article distributed under the terms and conditions of the Creative Commons Attribution (CC BY) license (<https://creativecommons.org/licenses/by/4.0/>).

**Abstract:** Ferromagnetic element ( $x = \text{Fe, Co, Ni, and Nd}$ )-promoted Pt/AC catalysts were prepared by co-impregnation method or physical mixing and tested in the liquid-phase hydrogenation of furfural to furfuryl alcohol (FA) under mild conditions (50 °C and 20 bar  $\text{H}_2$ ) using water and methanol as the solvent. Among the various catalysts studied, the 0.15FePt/AC exhibited complete conversion of furfural with an FA selectivity of 74% after only 1 h of reaction time in water. The promotional effect of the bimetallic catalysts became less pronounced when methanol was used as the solvent and a 2-furaldehyde dimethyl acetal solvent product was formed. The superior catalyst performances were correlated with the higher Pt dispersion, the presence of low coordination Pt sites, and the strong Pt–Fe interaction as characterized by X-ray diffraction,  $\text{H}_2$  temperature-programmed reduction ( $\text{H}_2$ -TPR),  $\text{N}_2$  physisorption, and infrared spectroscopy of the adsorbed CO (CO-IR). However, to simply use a magnet for catalyst separation, 0.5 wt% Fe was the minimum Fe loading on the Pt/AC. The 0.5FePt/AC still exhibited good magnetic properties after the third consecutive runs.

**Keywords:** furfural; furfuryl alcohol; hydrogenation; water and methanol; platinum-based catalysts

## 1. Introduction

The energy crisis and environmental pollution have currently been confronting human life due to increasing global energy consumption. Alternative energy resources such as solar, hydropower, wind, geothermal, and biomass have been extensively explored. Renewable biomass is a promising resource to use as feedstock instead of fossil fuel for the production of many petrochemical products. Furfural, a biomass-derived chemical produced by the acid-catalyzed dehydration of xylose [1], can be converted into a wide range of value-added derivative molecules [2]. Approximately 62% of the furfural produced is transformed into furfuryl alcohol (FA) by selective hydrogenation reaction [3]. FA is an interesting high-value chemical and important chemical in the fine chemical industry of lubricants, adhesives, drug intermediates, and dispersing agents and in the polymer industry of phenolic resin, furfural resin, and furan resin [4].

The selective hydrogenation of furfural to FA is an interesting reaction because furfural contains two powerful functional groups, an aldehyde ( $\text{C}=\text{O}$ ) and a conjugated system

(C=C–C=C) [2]. To produce FA, furfural is hydrogenated at the aldehyde group (C=O) and then transformed into FA. The catalytic hydrogenation of furfural to FA is usually performed either in the gas or liquid phase [5–8]. Compared to the gas-phase hydrogenation process, liquid-phase hydrogenation of furfural has the advantages of high selectivity and low energy consumption [9]. In the present industrial processes of furfural production, copper chromite (Cu–Cr) is being used as the catalyst for both liquid-phase and gas-phase furfural hydrogenation [10], performing under high-temperature (between 130 and 200 °C) and high-pressure (up to 30 bar) conditions. Although copper chromite exhibits good activity and selectivity toward FA, serious environmental pollution due to toxicity of Cr species is being concerned [11]. A variety of Cr-free catalysts have been investigated, including precious metal catalysts such as Pt [11–16], Ru [17,18], and Pd [19,20] and nonprecious metal catalysts such as Co [21], Cu [22,23], and Ni [24,25]. Among these catalysts, Pt exhibits good catalytic performances for selective hydrogenation of furfural to FA under mild conditions. The addition of a second metal including Co, Ni, and Fe has resulted in significant improvement of Pt-based catalysts for FA production. Liu et al. [26] prepared a bimetallic catalyst by adding Fe, Co, and Ni as promoters by a co-impregnation method and tested in the hydrogenation of furfural at 100 °C, 30 bar H<sub>2</sub> for 5 h. All the promoters exhibited a positive effect on furfural hydrogenation, especially Fe and Ni, in which furfural conversion and FA and tetrahydrofurfuryl alcohol (THFA) selectivity were significantly improved. Tolek et al. [27] reported the performances of bimetallic PtCo/TiO<sub>2</sub> with 0.7 wt% Pt and 0–0.4 wt% Co selective furfural hydrogenation to FA. The Pt-0.2Co/TiO<sub>2</sub> catalyst showed the best performance with 100% conversion of furfural and 97.5% selectivity towards FA. Dohade and Dhepe [28] also indicated that Pt–Co supported on activated carbon presented the most improved activity compared to the monometallic catalyst when the reaction was carried out at 180 °C for 8 h. Although the improvement of Pt catalysts promoted by ferromagnetic elements such as Fe and Ni as promoters for Pt catalysts in the hydrogenation of furfural to FA has been demonstrated, the comparison of the catalytic performances among them as well as their magnetic properties have been reported to a lesser extent, especially under different solvents. In the liquid-phase reaction, carbon powders are extremely difficult to separate from the solution and typically require complex and expensive steps such as filtration or centrifugation. The magnetic properties of catalysts make catalyst separation easy by using a simple external magnet. The magnetic properties of catalysts have been utilized in the hydrogenation of furfural to furfuryl alcohol over a Ni–Fe alloy [29] and Fe(NiFe)O<sub>4</sub>–SiO<sub>2</sub> nanoparticle catalysts [30]. Both catalytic and magnetic properties of carbon-supported Pt catalysts with ferromagnetic element promoters have not yet been reported.

In this work, we aimed to compare the liquid-phase hydrogenation of furfural to FA using various ferromagnetic elements (x = Fe, Co, Ni, and Nd)-promoted Pt/activated carbon catalysts under relatively mild reaction conditions (50 °C and 20 bar H<sub>2</sub>) using water and methanol as the solvent. The structural–activity relationship was investigated by means of X-ray diffraction, H<sub>2</sub> temperature-programmed reduction (H<sub>2</sub>-TPR), N<sub>2</sub> physisorption, and infrared spectroscopy of the adsorbed CO (CO-IR). The magnetic properties and reusability of the catalysts were also discussed.

## 2. Experimental

### 2.1. Catalyst Preparation

The Pt/AC (0.5 wt%), FePt/AC (0.5 wt% Pt and 0.1–10 wt% Fe), and 0.15MPt/AC (0.5 wt% Pt and 0.15 wt% M: Ni and Co) were prepared by co-impregnation method using commercial activated carbon (C = 90.81%, O = 9.02% and P = 0.18%), tetraammineplatinum (II) chloride hydrate ((Pt (NH<sub>3</sub>)<sub>4</sub>Cl<sub>2</sub>·xH<sub>2</sub>O), 99.99%, Sigma-Aldrich, Darmstadt, Germany), ferric nitrate nonahydrate (FeN<sub>3</sub>O<sub>9</sub>·9H<sub>2</sub>O, ≥97.0%, Fluka, Buchs, Switzerland), cobalt (II) nitrate hexahydrate (Co(NO<sub>3</sub>)<sub>2</sub>·6H<sub>2</sub>O, ≥98.0%, Carlo Erba, Milano, Italy), and nickel (II) nitrate hexahydrate (Ni(NO<sub>3</sub>)<sub>2</sub>·6H<sub>2</sub>O, ≥98.0%, ACS, Darmstadt, Germany), as C, Pt, Fe, Co, and Ni precursors, respectively. The Pt and the second metal precursors were dissolved in

deionized water, and then the aqueous solution was slowly dropped onto the activated carbon. The impregnated catalysts were dried overnight at 110 °C in an oven. Finally, the catalysts were calcined in N<sub>2</sub> at 500 °C for 2 h. The catalysts were denoted as Pt/AC and xMPt/AC when x was wt% and M was the second metal. The 0.15NdPt/AC (0.5 wt% Pt and 0.15 wt% Nd) was prepared by physical mixing. Firstly, the Pt/AC catalyst from impregnation was mixed with neodymium powder (<400 μm, Nd ≥ 99.0%, Sigma-Aldrich, Darmstadt, Germany) in toluene at room temperature and stirred for 40 min for uniform mixing. The solvent was removed from the mixture by centrifugation and washed by DI water. Then, the solid catalyst was dried at 110 °C overnight and calcined at 500 °C for 2 h in N<sub>2</sub> flow. The catalysts were denoted as 0.15NdPt/AC.

## 2.2. Catalyst Characterization

The H<sub>2</sub>-TPR measurements were carried out to determine reducibility and reduction temperature of the Pt-based catalysts. A quartz U-tube reactor was used, and all the catalyst samples were pretreated with a N<sub>2</sub> flow (25 mL/min, 1 h, 150 °C). The TPR profiles were obtained by passing carrier gas (10% H<sub>2</sub> in nitrogen) through the catalyst samples (25 mL/min, ramping from room temperature to 800 °C at 10 °C/min). The BET (Brunauer–Emmett–Teller) surface area, average pore size diameter, and pore size distribution were determined by physisorption of N<sub>2</sub> using a Micromeritics ASAP 2020, Micromeritics Instrument, Norcross, U.S.A. The morphologies of the catalysts were determined by JEOL-6400 scanning electron microscope, JEOL, Tokyo, Japan, and the elemental distribution over the catalyst surface was determined by Link Isis Series 300 program energy dispersive X-ray spectroscopy, respectively. The XRD patterns were collected using a Bruker D8 Advance with a Ni filter and Cu K<sub>α</sub> radiation. The platinum active sites were determined by CO pulse chemisorption technique using a Micromeritics ChemiSorb 2750 (pulse chemisorption system), Micromeritics Instrument, Norcross, U.S.A. The FTIR spectra of adsorbed CO were collected using FTIR-620 spectrometer (JASCO, Tokyo, Japan) with a MCT detector at a wavenumber resolution of 2 cm<sup>-1</sup>. The sample was heated to 500 °C and reduced by H<sub>2</sub> for 2 h. The actual metal loadings were determined by inductive coupled plasma-optical emission spectroscopy (ICP-OES) technique.

## 2.3. Catalyst Activity

The catalyst activity was tested in liquid-phase selective hydrogenation of furfural to furfuryl alcohol. Reactions were performed in a 100 mL stainless steel autoclave reactor (JASCO, Tokyo, Japan). Prior to the catalyst test, the catalysts were reduced under H<sub>2</sub> flow (25 cm<sup>3</sup> /min) at 500 °C for 2 h. For the furfural hydrogenation reaction, approximately 50 mg of catalyst, 50 μL of furfural, and 10 mL of solvent were added into reactor. Then, reactor was purged with hydrogen three times for removing the air. After that, the reaction was performed at 50 °C, 2 MPa of H<sub>2</sub> under stirring. The hydrogenation of furfural was carried out at 50 °C for 2 h in methanol and 1 h in water. After completion of the reaction, the reactor was cooled to below room temperature with an ice-water mixture and depressurized carefully. For methanol solvent, the liquid products were analyzed by a gas chromatograph Shimadzu GC-2014 (Shimadzu, Kyoto, Japan) equipped with a flame ionization detector (FID), and the Rxt-5 capillary column with 30 M length and 0.32 mm inside diameter were used. Then, 0.2 μL was injected into the column and helium was used as a carrier gas. In the case of distilled water solvent, the liquid products were analyzed with high-performance liquid chromatography (Shimadzu 20A) equipped with column Aminex HPX-87H (300 × 7.8 mm). The injection volume was 10 μL, and the absorbance detector wavelength was set at 215 nm. The mobile phase was composed of 86% H<sub>3</sub>PO<sub>4</sub> 0.1 N and 14% acetonitrile (HPLC grade), and the flow rate was 0.4 mL min<sup>-1</sup>.

### 3. Results and Discussion

#### 3.1. Catalyst Characterization

The XRD patterns of Pt/AC and Pt-based bimetallic catalysts prepared by impregnation and physical mixing in the range of diffraction angles ( $2\theta$ ) between  $20^\circ$  and  $80^\circ$  are shown in Figure 1. The characteristic diffraction peaks at  $2\theta = 24.4^\circ$ ,  $35.5^\circ$ , and  $43.3^\circ$  could be attributed to graphitized activated carbon [31,32]. However, the higher intensity of the diffraction peak at  $2\theta = 35.5^\circ$  was clearly observed on 5FePt/AC and 10FePt/AC, which could possibly be due to the overlap of the diffraction peak of iron, which occurred at around  $35.7^\circ$  [33]. There were no characteristic diffraction peaks corresponding to platinum, cobalt, nickel, and neodymium species detected for all the catalysts due probably to the low amounts of metal present and/or high dispersion of these metals on the carbon supports and/or very the small crystallite size of these metal particles.

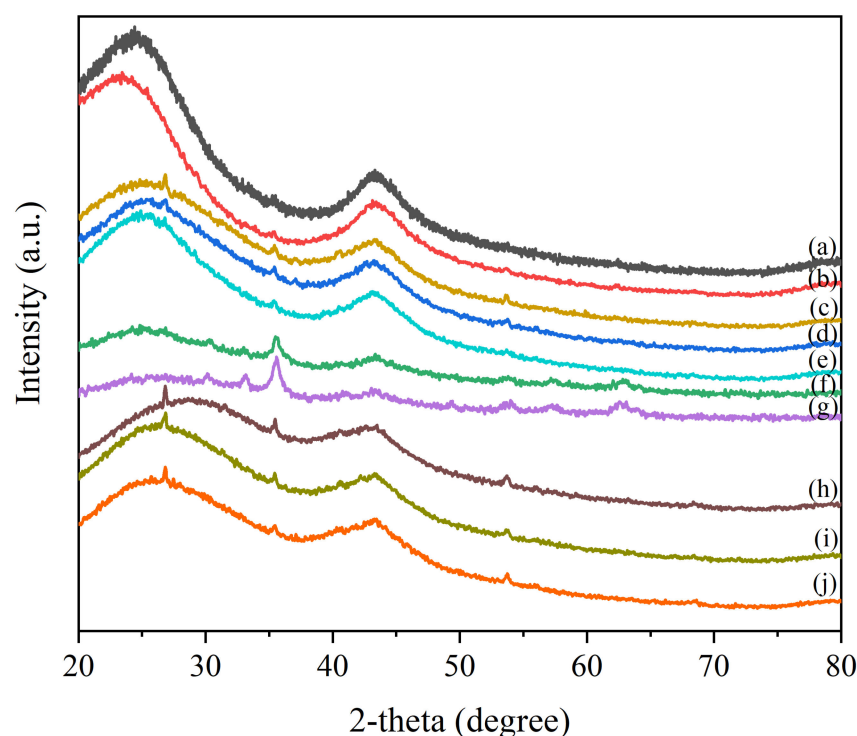


**Figure 1.** XRD pattern of Pt-based catalyst: (a) AC, (b) Pt/AC, (c) 0.1FePt/AC, (d) 0.15FePt/AC, (e) 0.2FePt/AC, (f) 5FePt/AC, (g) 10FePt/AC, (h) 0.15CoPt/AC, (i) 0.15NiPt/AC, and (j) 0.15NdPt/AC.

Nitrogen adsorption isotherms for the Pt/AC and Pt-based bimetallic catalysts are shown in Figure 2. All the catalyst samples exhibited type I isotherm, and the stepwise increase in the adsorption branch expressed the presence of both micropores and mesopores. The ICP-OES,  $N_2$  physisorption, and CO chemisorption results are given in Table 1. The actual loadings of Pt and the second metals were close to their nominal values. For a similar second-metal loading (e.g., 0.15MPt/AC), the calculated atomic ratios of Pt:M were in the range of 0.66–1.57. The BET surface area, the pore volume, and the pore diameters are summarized in Table 1. All the prepared supported carbon catalysts exhibited high surface area in the range of  $755$ – $988$   $m^2/g$ , with the 0.15FePt/AC having the highest surface area of  $988$   $m^2/g$ . For the lowest Fe loading 0.1FePt/AC, the BET surface area was not significantly different from the monometallic Pt/AC ( $804$  and  $793$   $m^2/g$ , respectively). The BET surface area of the bimetallic xMPt/AC ( $M = Fe, Co, \text{ and } Ni$ ) with  $x = 0.15$ – $5$  wt% was higher than that of Pt/AC. Such results suggest that the second metal may be highly dispersed as small particles on the external surface of the AC supports, which could create heterogeneity and roughness that led to an increased BET surface area. The Fe dispersion

would be maximized on the 0.15FePt/AC so that it exhibited the highest BET surface area (smallest Fe particles). As the Fe loading increased, larger Fe particles would form, and as the consequence the surface area decreased. The lowest BET surface area, 755 m<sup>2</sup>/g, was observed on the highest Fe loading 10FePt/AC.

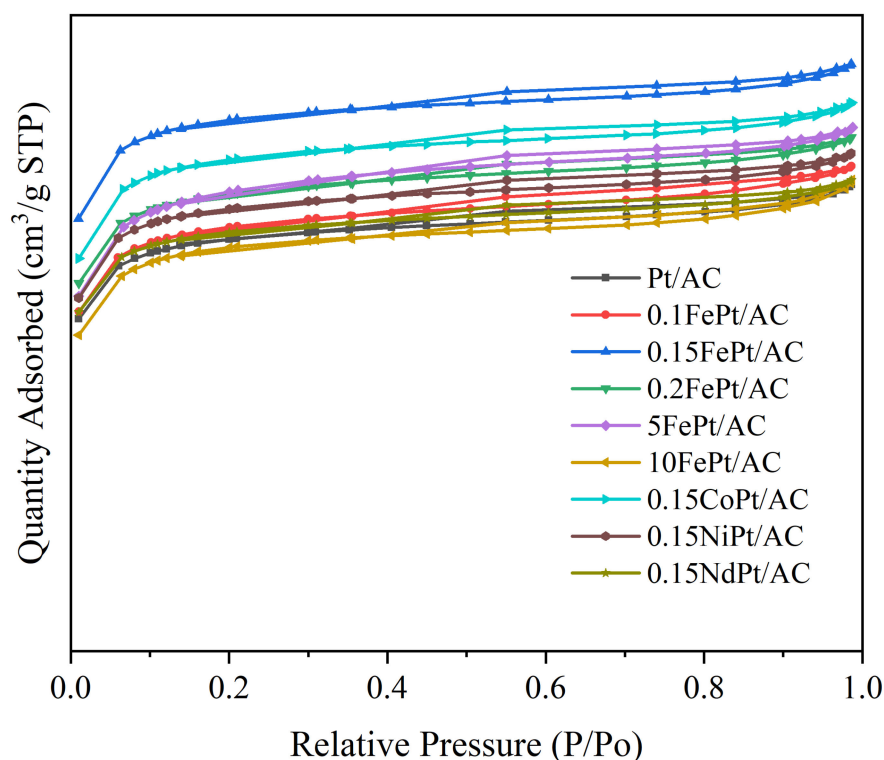


Figure 2. Nitrogen adsorption/desorption results of Pt-based catalysts.

Table 1. Atomic ratio, N<sub>2</sub> physisorption properties, CO-IR analysis, and active sites of Pt-based catalysts.

Catalyst	ICP Results (Metal Loading, wt%) <sup>a</sup>		Atomic Ratio (Pt/M) <sup>b</sup>	N <sub>2</sub> Physisorption Properties			The Ratio of CO Adsorption on Pt Atom at Edge Sites and Pt Terrace <sup>d</sup>	Active Sites (×10 <sup>18</sup> Molecule CO/g cat.) <sup>e</sup>
	Pt	M (M = Fe, Co, or Ni)		Surface Area (m <sup>2</sup> /g)	Pore Volume (cm <sup>3</sup> /g) <sup>c</sup>	Average Pore Size (nm) <sup>c</sup>		
Pt/AC	0.51	-	-	804	0.092	3.5	0.09	0.95
0.1FePt/AC	n.d.	n.d.	n.d.	793	0.110	3.4	n.d.	n.d.
0.15FePt/AC	0.53	0.23	0.66	988	0.102	3.2	0.47	5.69
0.2FePt/AC	n.d.	n.d.	n.d.	852	0.106	3.3	n.d.	n.d.
5FePt/AC	0.50	4.70	0.03	860	0.129	3.1	n.d.	n.d.
10FePt/AC	0.42	9.50	0.013	755	0.109	3.9	n.d.	n.d.
0.15CoPt/AC	0.52	0.10	1.57	915	0.104	3.4	0.21	2.94
0.15NiPt/AC	0.47	0.16	0.88	826	0.110	3.4	0.34	0.82
0.15NdPt/AC	0.48	n.d.	n.d.	780	0.094	3.5	0.16	1.85

n.d. = not determined. <sup>a</sup> Metal loading measured by ICP-OES. <sup>b</sup> Calculated from percentage of metal loading. <sup>c</sup> Calculated from BJH desorption method. <sup>d</sup> Based on CO-IR result. <sup>e</sup> Based on CO-chemisorption.

The morphologies and elemental distribution of the catalyst samples were investigated by SEM and EDX. The SEM images of Pt/AC and xMPt/AC are shown in Figure 3. All the catalysts showed non-uniform particle size and shape. There were no significant differences in the catalyst morphology when a second metal was added by co-impregnation and physical mixing technique. Moreover, the EDX results from the various 0.15MPt/AC

catalysts confirmed the existence of Pt, Fe, Co, Ni, and Nd on the catalyst surface and that the metal could be highly dispersed on the surface.

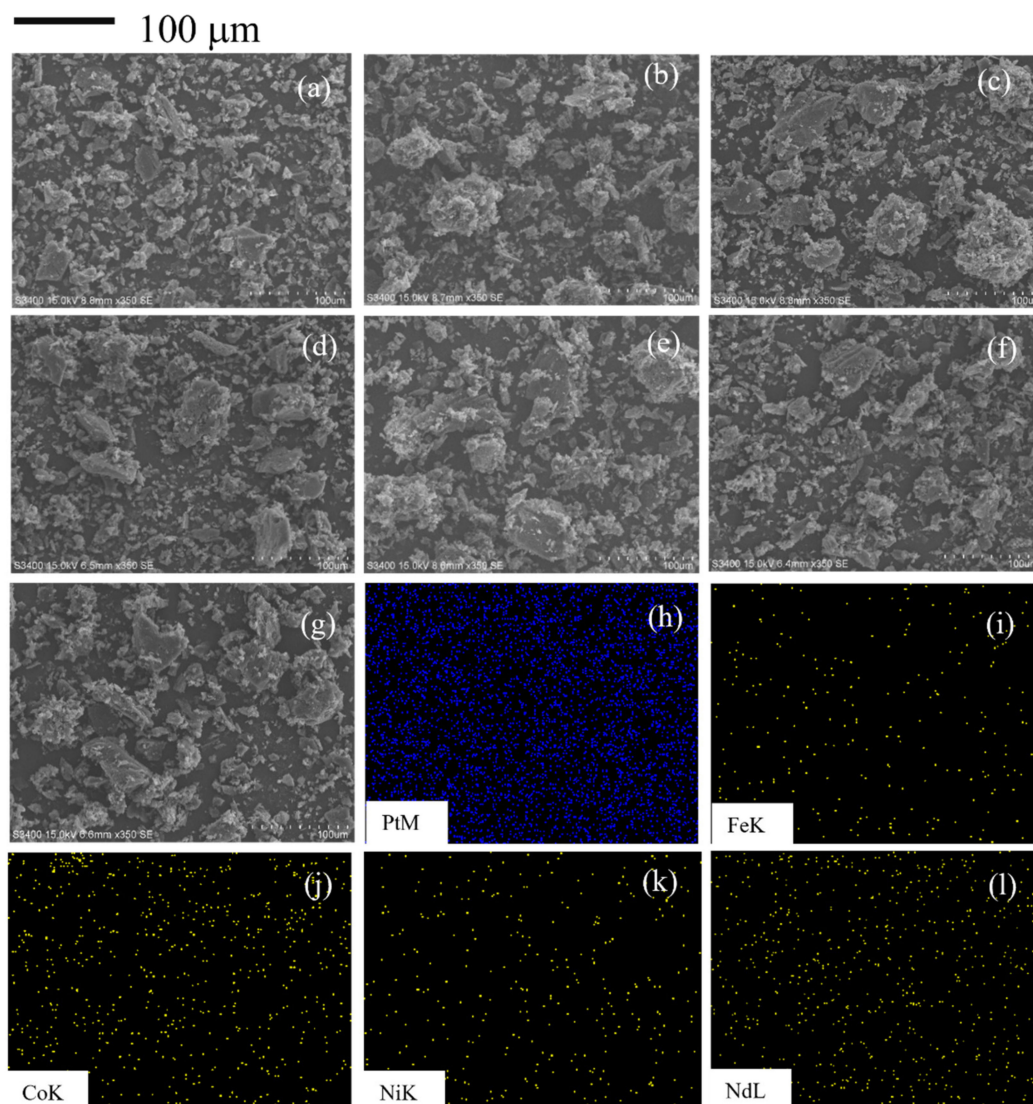


**Figure 3.** SEM images of (a) Pt/AC, (b) 0.15FePt/AC, (c) 5FePt/AC, (d) 10FePt/AC, (e) 0.15CoPt/AC, (f) 0.15NiPt/AC, and (g) 0.15NdPt/AC catalysts and the corresponding elemental mapping images of (h) platinum, (i) iron, (j) cobalt, (k) nickel, and (l) neodymium on 0.15MPt/AC.

The magnetic properties were tested by using a simple external magnet to separate the catalyst from liquid media (Figure 4). The efficiency of the magnetic separation is highly dependent on the amount of ferromagnetic elements. The minimum %wt. of Fe loading on the Pt/AC to make the catalyst separable from the liquid by a magnet was determined to be 0.5 wt% Fe. The superior catalyst separation by magnet is demonstrated for higher Fe loadings such as 5% and 10% of Fe loadings.

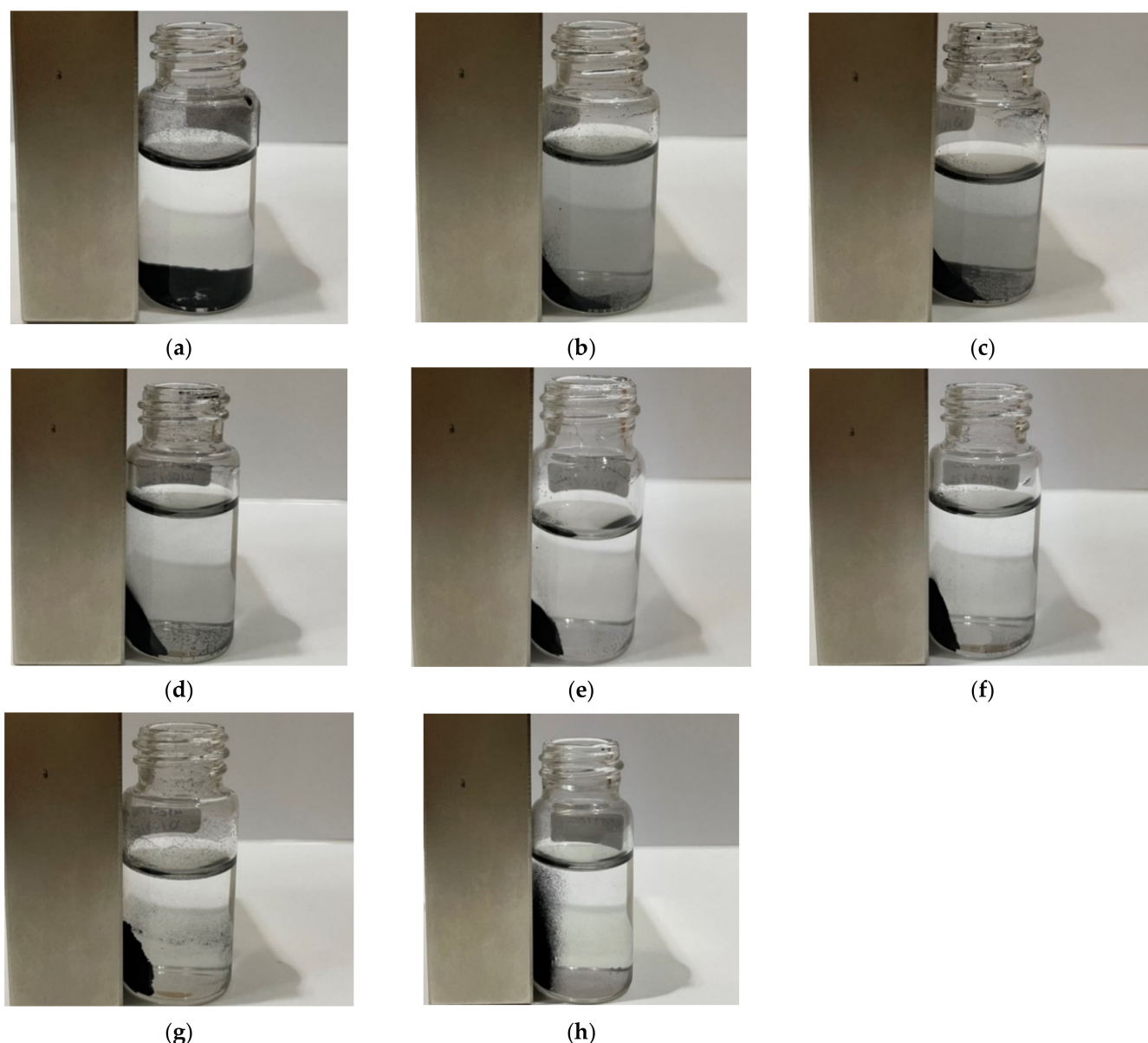


**Figure 4.** Magnetic separation of (a) 0.15FePt /AC, (b) 0.5FePt/AC, (c) 1FePt/AC, (d) 2FePt/AC, (e) 3FePt/AC, (f) 4FePt/AC, (g) 5FePt/AC, and (h) 10FePt/AC.

The characteristic of the surface of dispersed Pt particles was further studied by FTIR of the adsorbed CO on the Pt/AC and Pt-based bimetallic catalysts (Figure 5). The CO adsorption band at around  $2070\text{--}2100\text{ cm}^{-1}$  suggests a linear type of CO adsorption [34], and it has been reported that linear-type adsorbed CO dominated on small Pt particles [35]. For the Pt/AC, the adsorption band at  $2108\text{ cm}^{-1}$  could be attributed to the CO adsorbed on a coordinated Pt surface such as Pt(111) and Pt(100), whereas the band at  $2070\text{ cm}^{-1}$  was attributed to the low coordinated Pt sites such as the edge, kink, and corner ones. For all the bimetallic catalysts, the adsorption bands of both positions were slightly shifted towards a higher wavenumber compared to that of Pt/AC. The ratios of CO adsorption on low coordination Pt atoms at edge sites and Pt terrace (111) and (100) are given in Table 1. It can be seen that all the bimetallic catalysts exhibited larger relative quantity of less-coordinated Pt atoms on the edge, kink, and corner, especially for the 0.15 FePt/AC catalyst. In addition, the IR spectra relating to CO adsorbed species of Fe, Co, Ni, and Nd were not detected. Such results are similar to those previously reported by Einaga et al. [36] and Pisduangdaw et al. [37].

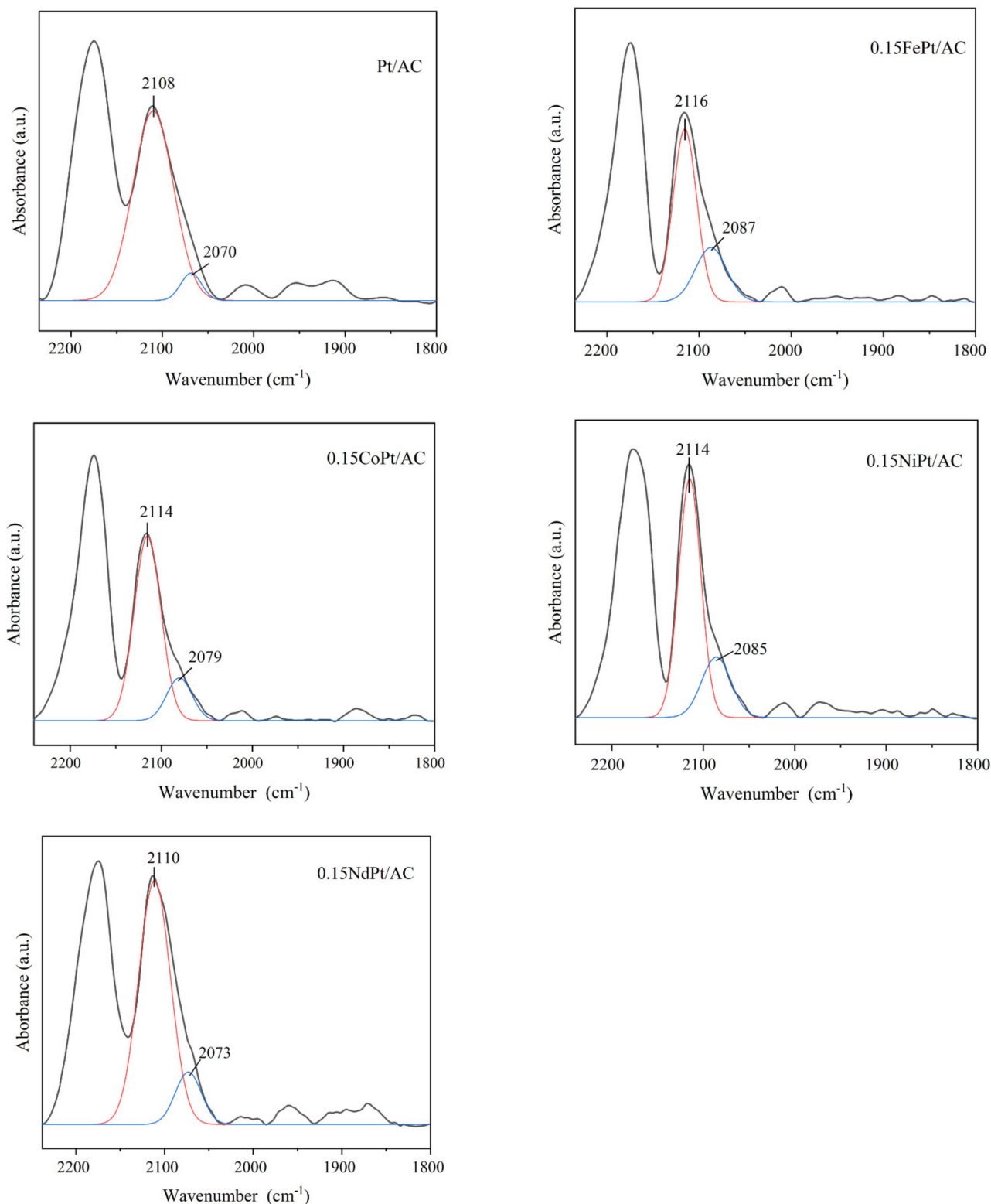


**Figure 5.** CO-IR result of the Pt-based catalysts.

The amounts of CO chemisorption on the Pt/AC and 0.15MPt/AC catalyst are demonstrated in Table 1. The number of surface Pt-active atoms on all the Pt catalysts derived from the CO uptake are ranging between  $0.82\text{--}5.69 \times 10^{18}$  molecules of CO in the order: 0.15FePt/AC > 0.15CoPt/AC > 0.15NdPt/AC > Pt/AC > 0.15NiPt/AC. The relatively low

CO uptake on 0.15NiPt/AC may be due to the partial coverage of the second metal on the Pt surface and/or alloy formation, resulting in a low amount of active Pt surface.

The H<sub>2</sub>-TPR measurements were carried out to study the reduction behaviors of the monometallic Pt/AC and bimetallic 0.15MPt/AC catalysts, and the results are shown in Figure 6. Both monometallic Pt/AC and bimetallic 0.15MPt/AC catalysts exhibited three reduction peaks at 230–270 °C, 300–350 °C, and 370–700 °C. The first reduction peak of the Pt/AC catalyst was associated with the reduction of Pt oxide to Pt metal [16]. When the second metals Fe, Co, Ni, and Nd were introduced into the monometallic Pt catalysts, the reduction temperature for PtO<sub>x</sub> was lower due probably to the formation of smaller Pt oxide particles (higher Pt dispersion) and/or the interaction between the second metal and Pt in the bimetallic catalysts [9]. The second reduction peak was typically correlated to the reduction of Pt species interacting with the carbon support. Among the various ferromagnetic-element-promoted Pt/AC catalysts, the second reduction peak was higher and shifted to a higher reduction temperature only when Fe was added, which indicated a stronger interaction between the metal and carbon support and/or a Pt–Fe alloy [26]. The third reduction peaks were the carbon gasification process to form CH<sub>4</sub>. It had been reported that the formation of methane generally occurs in the temperature range of 390–800 °C [26].

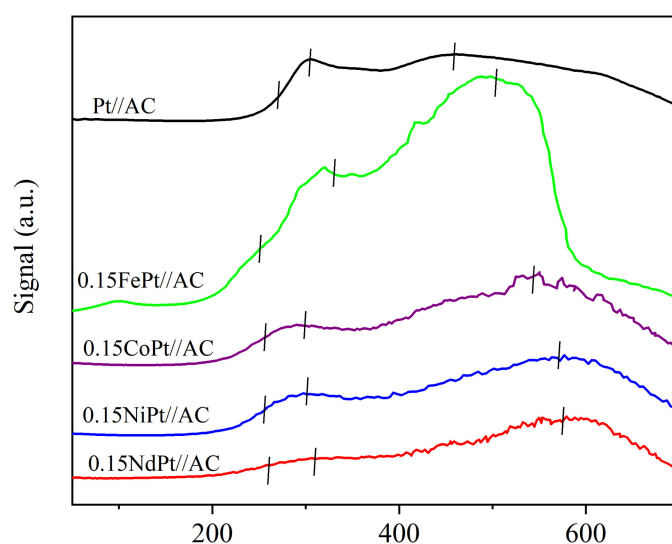


**Figure 6.** H<sub>2</sub> temperature-programmed reduction profiles of the catalysts.

### 3.2. Catalytic Reaction Study

The catalytic activities of the prepared catalysts were evaluated in the liquid-phase hydrogenation of furfural to furfuryl alcohol under mild reaction conditions (temperature of 50 °C and H<sub>2</sub> pressure of 2 MPa). All the catalysts were reduced at 500 °C in H<sub>2</sub> flow for 2 h before the reaction test. In a liquid-phase reaction, the choice of solvent usually has an impact on the catalytic activity [13]. In this study, methanol and water were used as the medium to investigate the solvent effect in the hydrogenation of furfural, and the results are summarized in Table 2. The addition of ferromagnetic metal on the Pt/AC catalysts showed different effects on the catalytic performances in the furfural hydrogenation, depending on the solvent used. Using methanol as the solvent, a slight improvement on the FA yield was found on the 0.15%FePt/AC catalyst (36.4%) compared to the Pt/AC (31.3%). Whilst the other bimetallic 0.15%CoPt/AC and 0.15%NiPt/AC catalysts exhibited much lower FA yields at 22.3% and 11.3%, respectively. In addition, the furfural conversion and FA selectivity decreased with increasing Fe loading from 0.15 to 5 and 10 wt%, especially for the 10FePt/AC that showed the lowest performance. Besides, the 2-furaldehyde dimethyl acetal solvent product (SP), which is the side reaction product that occurred from the methanol reacted with furfural, was found when using methanol as the solvent. SP was

normally observed in alcohols solvent, not only methanol but also ethanol, isopropanol, etc. [11,13]. The other by-products include 2-methylfuran and 1-pentanol, which were formed via hydrogenolysis of FA and ring-opening of 2-methylfuran, respectively [2].

**Table 2.** Catalytic reaction of the selective hydrogenation of furfural to furfuryl alcohol over the prepared catalysts.

Catalyst	Solvent	Reaction Time (h)	Conversion (%)	Selectivity (%)		
				FA	SP	Others <sup>a</sup>
Pt/AC	Methanol	2	53.9	58.0	4.1	37.9
0.15FePt/AC	Methanol	2	64.1	56.8	6.0	37.2
5FePt/AC	Methanol	2	47.6	10.4	1.1	88.5
10FePt/AC	Methanol	2	14.1	0	7.0	93.0
0.15CoPt/AC	Methanol	2	62.9	35.4	1.5	63.1
0.15NiPt/AC	Methanol	2	26.7	42.4	21.3	36.3
Pt/AC	Water	1	81.8	45.2	-	54.8
0.1FePt/AC	Water	1	100	57.4	-	42.6
0.15FePt/AC	Water	1	100	74.1	-	25.9
0.2FePt/AC	Water	1	91.9	65.6	-	34.4
0.5FePt/AC	Water	1	95.9	58.1	-	41.9
5FePt/AC	Water	1	83.6	56.6	-	43.4
10FePt/AC	Water	1	58.4	41.4	-	58.6
0.15CoPt/AC	Water	1	88.1	47.6	-	52.4
0.15NiPt/AC	Water	1	96.7	32.6	-	67.4
0.15NdPt/AC	Water	1	75.5	32.6	-	67.4

Reaction (50  $\mu$ L furfural in 10 mL solvent) at 50 °C with a 50 mg catalyst under 2 MPa of H<sub>2</sub> for 120 min in methanol and 60 min in water and catalysts were reduced at 500 °C, 2 h in H<sub>2</sub> flow. <sup>a</sup> Based on GC–MS analysis, the by-products include 2-methylfuran and 1-pentanol.

The catalytic activity of various amounts of Fe loading and other bimetallic 0.15MPt/AC catalysts was also examined in the aqueous-phase hydrogenation of furfural to FA at 50 °C and 2 MPa H<sub>2</sub>, 1 h reaction time using water as the solvent (Table 2). Unlike the use of methanol solvent, when the reaction was carried out in water, all the PtFe/AC showed higher furfural conversion than the monometallic Pt/AC, except for the 10FePt/AC. The conversion of furfural varied in the order: 0.15FePt/AC (100%) = 0.1FePt/AC (100%) > 0.2FePt/AC (91.9%) > 5FePt/AC (83.6%) > Pt/AC (81.8%) >> 10FePt/AC (58.4%). In addition, the FA selectivity decreased in the order: 0.15FePt/AC (74.1%) > 0.2FePt/AC (65.6%) > 0.1FePt/AC (57.4%) > 5FePt/AC (56.6%) > Pt/AC (45.2%) ~ 10FePt/AC (41.4%). The results indicated that the xFePt/AC series with the small amount of Fe (0.1–0.5 wt%) could improve both furfural conversion and FA selectivity of the Pt/AC catalysts, especially in water solvent. The superior catalyst performances were attributed to high Pt dispersion and a strong interaction between Pt and the carbon support and/or the formation of a Pt–Fe alloy [26,38]. The role of Fe to enhance the selectivity of carbonyl compound (C=O) reduction has been suggested by Ananthan S.A. et al. that Pt–Fe sites favored the di- $\sigma$ CO adsorption, which promoted the activation of the C=O group over the supported Pt–Fe catalysts [39].

Furthermore, the catalytic performances of Pt/AC, 0.15FePt/AC, 0.15CoPt/AC, 0.15NiPt/AC, and 0.15NdPt/AC were also investigated in water solvent. The hydrogenation of furfural to FA can occur from hydrogenation of the aldehyde group (C=O). The conversion of furfural of the Pt-based bimetallic catalysts were ranged between 75.5–100%. Improvement in furfural conversion by co-impregnation was correlated to high Pt dispersion with higher Pt active sites as determined by CO chemisorption. Surprisingly, 0.15NdPt/AC with higher Pt sites results revealed lower hydrogenation activity in the furfural hydrogenation than the monometallic Pt/AC. It is likely that the physical mixing of Nd power and Pt/AC catalyst led to poor Pt–Nd interaction. From the H<sub>2</sub>-TPR, the second reduction peak, which was attributed to the Pt species that strongly interacted with the support, became flattened on the 0.15NdPt/AC. In other words, the addition of Nd could weaken the Pt–support

interaction. Hence, the catalyst was less active under the reaction conditions despite its high dispersion. The FA selectivity of all the other 0.15 MPt/AC catalysts (Co, Ni, Nd) was not much different at around 32.6–47.6% and was similar to those obtained on the monometallic Pt/AC catalyst (45.2%). The highest conversion of furfural and FA selectivity on the 0.15FePt/AC was in accordance with the high dispersion with high Pt active sites and the strongest Pt–Fe or Pt–C interaction and/or a Pt–Fe alloy as indicated by the shift of the reduction temperature in the H<sub>2</sub>-TPR profiles. Moreover, the hydrogenation of the aldehyde group (C=O) would preferentially proceed on less-coordinated Pt sites such as the edge, corner, and kink.

Considering the solvent effect between methanol and water on all the Pt-based bimetallic catalysts, the use of water exhibited higher conversion and selectivity than methanol, although a shorter reaction time was used (1 h). It can be concluded that the activity and product selectivity in furfural hydrogenation over Pt-based bimetallic catalysts were promoted by the higher polar solvent. It is generally accepted that hydrogenation of  $\alpha$ - and  $\beta$ -unsaturated aldehydes is controlled by hydrogen solubility, solvent polarity, and the interaction between the catalyst and solvent [40]. A comparison between the Pt-based catalyst in this study and those reported in the literature is summarized in Table 3. At state-of-the-art, the highest furfural conversion (>99%) with FA selectivity (>99%) could be obtained on the Pt/NC-BS-500 catalyst in water solvent but under more severe conditions (100 °C and 2 MPa H<sub>2</sub>), longer reaction time (4 h), and higher amount of Pt loading (5 wt%) [16]. The carbon support material from bamboo shoots was prepared in two steps, including a hydrothermal treatment and a carbonization process, and Pt-supported on carbon was prepared using an ultrasound-assisted reduction method. The catalysts in this study achieved similar conversion with relatively high FA selectivity under milder reaction conditions. The beneficial effect of water solvent was also emphasized.

**Table 3.** Comparison of the prepared catalysts and reported in the literature for the liquid-phase hydrogenation of furfural.

No.	Catalysts	Preparation Method	Reaction Conditions	Solvent	Reaction Time (h)	Reaction Results		Ref.
						Conversion (%)	Selectivity (%)	
1	0.15FePt/AC	Co-impregnation	50 °C, 2 MPa H <sub>2</sub>	H <sub>2</sub> O	1	100	74.1	This work
	Pt-Fe/MWNT	Co-impregnation	100 °C, 3 MPa H <sub>2</sub>	Ethanol	5	95.2	91.8	
	Pt-Fe/H-AC	Co-impregnation	100 °C, 10.3 MPa H <sub>2</sub>	Ethanol	5	35.5	33.4	
2	Pt-Fe/AC	Co-impregnation	100 °C, 10.3 MPa H <sub>2</sub>	Ethanol	5	52.9	28.6	[26]
	Pt-Ni/MWNT	Co-impregnation	100 °C, 10.3 MPa H <sub>2</sub>	Ethanol	5	95.9	84.1	
	Pt-Co/MWNT	Co-impregnation	100 °C, 10.3 MPa H <sub>2</sub>	Ethanol	5	86.7	80.3	
3	5%Pt@TECN	Ultrasound-assisted reduction	100 °C, 1 MPa H <sub>2</sub>	H <sub>2</sub> O	5	>99	>99	[13]
	5%Pt@TECN	Ultrasound-assisted reduction	100 °C, 2 MPa H <sub>2</sub>	H <sub>2</sub> O	1	98	98	
4	3%Pt/BC	Wet impregnation	210 °C, 10.3 MPa H <sub>2</sub>	Toluene	2	60.8	79.2	[41]
5	3%Pt/AC	Wet impregnation	180 °C, 1 MPa H <sub>2</sub>	Isopropanol	8	100	71	[28]
6	Pt/NC-BS-500	Ultrasound-assisted reduction	100 °C, 1 MPa H <sub>2</sub>	H <sub>2</sub> O	4	>99	>99	[16]
7	Pt-Sn <sub>0.3</sub> /SiO <sub>2</sub>	Controlled surface reaction	100 °C, 1 MPa H <sub>2</sub>	2-propanol	8	>90	96.2	[12]
8	Pt-Re/TiO <sub>2</sub> -ZrO <sub>2</sub>	Co-impregnation	130 °C, 5 MPa H <sub>2</sub>	Ethanol	8	100	95.7	[42]
	Pt-In/TiO <sub>2</sub> -ZrO <sub>2</sub>	Co-impregnation	130 °C, 5 MPa H <sub>2</sub>	Ethanol	8	73.3	74.9	
	Pt-Sn/TiO <sub>2</sub> -ZrO <sub>2</sub>	Co-impregnation	130 °C, 5 MPa H <sub>2</sub>	Ethanol	8	98.3	47.8	

The 0.5FePt/AC catalyst was chosen for recyclability tests because it contained the minimum loading of Fe that made the catalyst separable from the liquid by a magnet. The results are shown in Figure 7. After the reaction, the catalyst was separated by a magnet, washed with DI water three times, dried in an oven at 110 °C overnight, and used under the same reaction conditions in water solvent. It was found that the conversion of furfural and FA selectivity decreased after the first run but were not significantly changed in the consecutive run. During the first run, some large Pt particles with weak metal–support interaction could be leached out from the carbon support. Comparison of the EDX of the fresh and spent catalyst after the third run is shown in Table 4. The differences in the O/C ratios suggest the deposition of carbon species from the liquid phase under the conditions used. The XPS results of C 1s (Table 5) also suggest the increase of C–O–C and O–C=O species on the spent catalysts compared to the fresh one, of which more than 90% was C–C species [43]. The Fe 2p peaks on both fresh and spent catalysts at around 711.2–711.4 eV were attributed to Fe<sup>3+</sup> in Fe<sub>2</sub>O<sub>3</sub> [44], and the amounts were not significantly different (<1 wt%). After the third cycle run, the 0.5FePt/AC catalyst still maintained the magnetic properties and could be separated by a magnet (Figure 8).

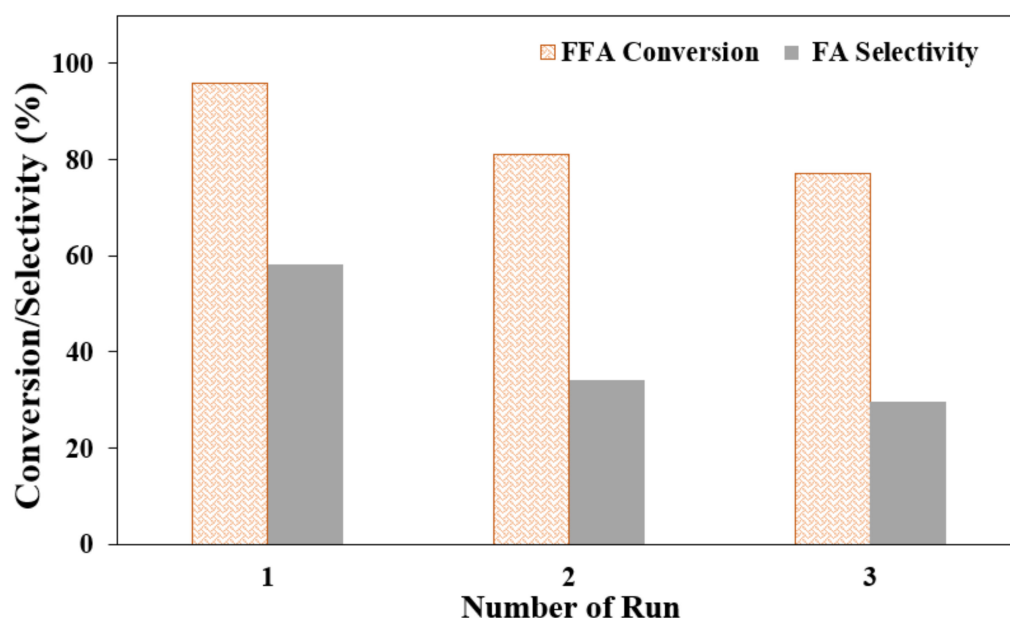


Figure 7. Catalyst recyclability with the 0.5FePt/AC catalysts for the conversion of furfural to furfuryl alcohol.

Table 4. EDX results of fresh and spent 0.5 FePt/AC catalysts after 3rd cycle.

0.5FePt/AC	EDX (wt%)				Ratio O/C
	C	O	Pt	Fe	
Fresh	90.57	6.42	1.86	1.9	0.066
Spent 3rd cycle	94.2	3.41	1.64	0.79	0.036

**Table 5.** XPS results of fresh and spent 0.5 FePt/AC catalysts after 3rd cycle.

	Fresh		After 3rd Cycle	
	Binding Energy (eV)	Mass (%)	Binding Energy (eV)	Mass (%)
C 1s	285.0	68.71	285.0	43.39
	288.9	6.57	286.6	26.89
			288.7	12.60
O 1s	533.7	24.30	533.4	16.23
Fe 2p	711.4	0.42	711.2	0.90
Ratio O/C		0.323		0.196

**Figure 8.** Magnetic separation of 0.5FePt/AC catalyst (a) after 1st cycle run and (b) after 3rd cycle run.

#### 4. Conclusions

The liquid-phase selective hydrogenation of furfural to FA under mild conditions (50 °C and 20 bar H<sub>2</sub>) was studied over various ferromagnetic elements (x = Fe, Co, Ni, and Nd)-promoted Pt/activated carbon catalysts. Among the ferromagnetic elements, the 0.15FePt/AC catalyst exhibited the best improvement of catalyst performances in terms of FA yield in both methanol and water solvent, which was attributed to the highest Pt dispersion with low coordinated Pt sites, and the strong Pt–Fe interaction as revealed by CO chemisorption and FTIR of the adsorbed CO results. The highest FA yield was 74% in water. For all the Pt-based bimetallic catalysts, the use of water medium showed higher furfural conversion and FA selectivity than methanol, despite a shorter reaction time used (1 h). The minimum Fe loading was 0.5 wt% to make the bimetallic catalysts separable by a simple magnet. The activities and selectivity of the 0.5FePt/AC slightly dropped after the first cycle but remained stable afterward. The catalysts, however, still exhibited magnetic properties after the consecutive runs.

**Author Contributions:** S.S.: Methodology, Investigation, Formal analysis, Writing—original draft, P.W.: Formal analysis, L.C.: Resources, Formal analysis, Supervision, P.P.: Resources, J.P.: Supervision, Conceptualization, Formal analysis, Writing—review and editing, Funding acquisition. All authors have read and agreed to the published version of the manuscript.

**Funding:** National Research Council of Thailand (NRCT)—Research Team Promotion grant—Joongjai Panpraont, the Thailand Science Research and Innovation (IRN62W00001).

**Acknowledgments:** The financial supports from the National Research Council of Thailand (Research Team Promotion Grant-Joongjai Panpraont) and the Thailand Science Research and Innovation (IRN62W0001) are gratefully acknowledged.

**Conflicts of Interest:** The authors declare no conflict of interest.

## References

1. Mariscal, R.; Maireles-Torres, P.; Ojeda, M.; Sádaba, I.; Granados, M.L. Furfural: A renewable and versatile platform molecule for the synthesis of chemicals and fuels. *Energy Environ. Sci.* **2016**, *9*, 1144–1189. [[CrossRef](#)]
2. Yan, K.; Wu, G.; Lafleur, T.; Jarvis, C. Production, properties and catalytic hydrogenation of furfural to fuel additives and value-added chemicals. *Renew. Sustain. Energy Rev.* **2014**, *38*, 663–676. [[CrossRef](#)]
3. Peleteiro, S.; Rivas, S.; Alonso, J.L.; Santos, V.; Parajó, J.C. Furfural production using ionic liquids: A review. *Bioresour. Technol.* **2016**, *202*, 181–191. [[CrossRef](#)]
4. Sun, D.; Sato, S.; Ueda, W.; Primo, A.; Garcia, H.; Corma, A. Production of C4 and C5 alcohols from biomass-derived materials. *Green Chem.* **2016**, *18*, 2579–2597. [[CrossRef](#)]
5. Nagaraja, B.M.; Padmasri, A.H.; Raju, B.D.; Rao, K.R. Vapor phase selective hydrogenation of furfural to furfuryl alcohol over Cu–MgO coprecipitated catalysts. *J. Mol. Catal. A Chem.* **2007**, *265*, 90–97. [[CrossRef](#)]
6. Wu, J.; Shen, Y.; Liu, C.; Wang, H.; Geng, C.; Zhang, Z. Vapor phase hydrogenation of furfural to furfuryl alcohol over environmentally friendly Cu–Ca/SiO<sub>2</sub> catalyst. *Catal. Commun.* **2005**, *6*, 633–637. [[CrossRef](#)]
7. Sharma, R.V.; Das, U.; Sammynaiken, R.; Dalai, A.K. Liquid phase chemo-selective catalytic hydrogenation of furfural to furfuryl alcohol. *Appl. Catal. A Gen.* **2013**, *454*, 127–136. [[CrossRef](#)]
8. Yan, K.; Jarvis, C.; Lafleur, T.; Qiao, Y.; Xie, X. Novel synthesis of Pd nanoparticles for hydrogenation of biomass-derived platform chemicals showing enhanced catalytic performance. *RSC Adv.* **2013**, *3*, 25865–25871. [[CrossRef](#)]
9. Jia, P.; Lan, X.; Li, X.; Wang, T. Highly active and selective NiFe/SiO<sub>2</sub> bimetallic catalyst with optimized solvent effect for the liquid-phase hydrogenation of furfural to furfuryl alcohol. *ACS Sustain. Chem. Eng.* **2018**, *6*, 13287–13295. [[CrossRef](#)]
10. Jia, P.; Lan, X.; Li, X.; Wang, T. Deactivation mechanistic studies of copper chromite catalyst for selective hydrogenation of 2-furfuraldehyde. *J. Catal.* **2013**, *299*, 336–345.
11. Taylor, M.J.; Durndell, L.J.; Isaacs, M.A.; Parlett, C.M.; Wilson, K.; Lee, A.F.; Kyriakou, G. Highly selective hydrogenation of furfural over supported Pt nanoparticles under mild conditions. *Appl. Catal. B Environ.* **2016**, *180*, 580–585. [[CrossRef](#)]
12. Merlo, A.B.; Vetere, V.; Ruggera, J.F.; Casella, M.L. Bimetallic PtSn catalyst for the selective hydrogenation of furfural to furfuryl alcohol in liquid-phase. *Catal. Commun.* **2009**, *10*, 1665–1669. [[CrossRef](#)]
13. Chen, X.; Zhang, L.; Zhang, B.; Guo, X.; Mu, X. Highly selective hydrogenation of furfural to furfuryl alcohol over Pt nanoparticles supported on g-C<sub>3</sub>N<sub>4</sub> nanosheets catalysts in water. *Sci. Rep.* **2016**, *6*, 28558. [[CrossRef](#)]
14. Biradar, N.S.; Hengne, A.A.; Birajdar, S.N.; Swami, R.; Rode, C.V. Tailoring the product distribution with batch and continuous process options in catalytic hydrogenation of furfural. *Org. Process Res. Dev.* **2014**, *18*, 1434–1442. [[CrossRef](#)]
15. Wang, C.; Guo, Z.; Yang, Y.; Chang, J.; Borgna, A. Hydrogenation of furfural as model reaction of bio-oil stabilization under mild conditions using multiwalled carbon nanotube (MWNT)-supported Pt catalysts. *Ind. Eng. Chem. Res.* **2014**, *53*, 11284–11291. [[CrossRef](#)]
16. Liu, X.; Zhang, B.; Fei, B.; Chen, X.; Zhang, J.; Mu, X. Tunable and selective hydrogenation of furfural to furfuryl alcohol and cyclopentanone over Pt supported on biomass-derived porous heteroatom doped carbon. *Faraday Discuss* **2017**, *202*, 79–98. [[CrossRef](#)] [[PubMed](#)]
17. Aldosari, O.F.; Iqbal, S.; Miedziak, P.J.; Brett, G.L.; Jones, D.R.; Liu, X.; Edwards, J.K.; Morgan, D.J.; Knight, D.K.; Hutchings, G.J. Pd–Ru/TiO<sub>2</sub> catalyst—An active and selective catalyst for furfural hydrogenation. *Catal. Sci. Technol.* **2016**, *6*, 234–242. [[CrossRef](#)]
18. Musci, J.J.; Merlo, A.B.; Casella, M.L. Aqueous phase hydrogenation of furfural using carbon-supported Ru and RuSn catalysts. *Catal. Today* **2017**, *296*, 43–50. [[CrossRef](#)]
19. Garcia-Olmo, A.J.; Yopez, A.; Balu, A.M.; Prinsen, P.; Garcia, A.; Maziere, A.; Len, C.; Luque, R. Activity of continuous flow synthesized Pd-based nanocatalysts in the flow hydroconversion of furfural. *Tetrahedron* **2017**, *73*, 5599–5604. [[CrossRef](#)]
20. Lee, J.; Woo, J.; Nguyen-Huy, C.; Lee, M.S.; Joo, S.H.; An, K. Highly dispersed Pd catalysts supported on various carbons for furfural hydrogenation. *Catal. Today* **2020**, *350*, 71–79. [[CrossRef](#)]
21. Audemar, M.; Ciotonea, C.; De Oliveira Vigier, K.; Royer, S.; Ungureanu, A.; Dragoi, B.; Dumitriu, E.; Jérôme, D. Selective hydrogenation of furfural to furfuryl alcohol in the presence of a recyclable cobalt/SBA-15 catalyst. *ChemSusChem* **2015**, *8*, 1885–1891. [[CrossRef](#)] [[PubMed](#)]
22. Jiménez-Gómez, C.P.; Cecilia, J.A.; Moreno-Tost, R.; Maireles-Torres, P. Selective furfural hydrogenation to furfuryl alcohol using Cu-based catalysts supported on clay minerals. *Top. Catal.* **2017**, *60*, 1040–1053. [[CrossRef](#)]
23. Villaverde, M.M.; Bertero, N.M.; Garetto, T.F.; Marchi, A.J. Selective liquid-phase hydrogenation of furfural to furfuryl alcohol over Cu-based catalysts. *Catal. Today* **2013**, *213*, 87–92. [[CrossRef](#)]
24. Kotbagi, T.V.; Gurav, H.R.; Nagpure, A.S.; Chilukuri, S.V.; Bakker, M.G. Highly efficient nitrogen-doped hierarchically porous carbon supported Ni nanoparticles for the selective hydrogenation of furfural to furfuryl alcohol. *RSC Adv.* **2016**, *6*, 67662–67668. [[CrossRef](#)]
25. Gong, W.; Chen, C.; Zhang, H.; Zhang, Y.; Zhang, Y.; Wang, G.; Zhao, H. Highly selective liquid-phase hydrogenation of furfural over N-doped carbon supported metallic nickel catalyst under mild conditions. *Mol. Catal.* **2017**, *429*, 51–59. [[CrossRef](#)]
26. Liu, L.; Lou, H.; Chen, M. Selective hydrogenation of furfural over Pt based and Pd based bimetallic catalysts supported on modified multiwalled carbon nanotubes (MWNT). *Appl. Catal. A Gen.* **2018**, *550*, 1–10. [[CrossRef](#)]

27. Tolek, W.; Khruachao, K.; Pongthawornsakun, B.; Mekasuwandumrong, O.; Aires, F.J.C.S.; Weerachawanasak, P.; Panpranot, J. Flame spray-synthesized Pt-Co/TiO<sub>2</sub> catalysts for the selective hydrogenation of furfural to furfuryl alcohol. *Catal. Commun.* **2021**, *149*, 106246. [[CrossRef](#)]
28. Dohade, M.G.; Dhepe, P.L. One pot conversion of furfural to 2-methylfuran in the presence of PtCo bimetallic catalyst. *Clean Technol. Environ. Policy* **2017**, *20*, 703–713. [[CrossRef](#)]
29. Putro, W.S.; Hara, T.; Ichikuni, N.; Shimazu, S. Efficiently recyclable and easily separable Ni-Fe alloy catalysts for chemoselective hydrogenation of biomass-derived furfural. *Chem. Lett.* **2017**, *46*, 149–151. [[CrossRef](#)]
30. Halilu, A.; Ali, T.H.; Atta, A.Y.; Sudarsanam, P.; Bhargava, S.K.; Abd Hamid, S.B. Highly Selective hydrogenation of biomass-derived furfural into furfuryl alcohol using a novel magnetic nanoparticles catalyst. *Energy Fuels* **2016**, *30*, 2216–2226. [[CrossRef](#)]
31. Liu, X.-Y.; Huang, M.; Ma, H.-L.; Zhang, Z.-Q.; Gao, J.-M.; Zhu, Y.-L.; Han, X.-L.; Guo, X.-Y. Preparation of a carbon-based solid acid catalyst by sulfonating activated carbon in a chemical reduction process. *Molecules* **2010**, *15*, 7188–7196. [[CrossRef](#)] [[PubMed](#)]
32. Chen, H.; He, D.; He, Q.; Jiang, P.; Zhou, G.; Fu, W. Selective hydrogenation of p-chloronitrobenzene over an Fe promoted Pt/AC catalyst. *RSC Adv.* **2017**, *7*, 29143–29148. [[CrossRef](#)]
33. Dorniani, D.; Hussein, M.Z.B.; Kura, A.U.; Fakurazi, S.; Shaari, A.H.; Ahmad, Z. Preparation of Fe<sub>(3)</sub>O<sub>(4)</sub> magnetic nanoparticles coated with gallic acid for drug delivery. *Int. J. Nanomed.* **2012**, *7*, 5745–5756. [[CrossRef](#)] [[PubMed](#)]
34. Yoshida, H.; Igarashi, N.; Fujita, S.I.; Panpranot, J.; Arai, M. Influence of crystallite size of TiO<sub>2</sub> supports on the activity of dispersed pt catalysts in liquid-phase selective hydrogenation of 3-nitrostyrene, nitrobenzene, and styrene. *Catal. Lett.* **2014**, *145*, 606–611. [[CrossRef](#)]
35. Corma, A.; Serna, P.; Concepción, P.; Calvino, J.J. Transforming nonselective into chemoselective metal catalysts for the hydrogenation of substituted nitroaromatics. *J. Am. Chem. Soc.* **2008**, *130*, 8748–8753. [[CrossRef](#)] [[PubMed](#)]
36. Einaga, H.; Urahama, N.; Tou, A.; Teraoka, Y. CO oxidation over TiO<sub>2</sub>-supported Pt–Fe catalysts prepared by coimpregnation methods. *Catal. Lett.* **2014**, *144*, 1653–1660. [[CrossRef](#)]
37. Pisduangdaw, S.; Mekasuwandumrong, O.; Fujita, S.I.; Arai, M.; Yoshida, H.; Panpranot, J. One step synthesis of Pt–Co/TiO<sub>2</sub> catalysts by flame spray pyrolysis for the hydrogenation of 3-nitrostyrene. *Catal. Commun.* **2015**, *61*, 11–15. [[CrossRef](#)]
38. Da Silva, A.B.; Jordão, E.; Mendes, M.J.; Fouilloux, P. Selective hydrogenation of cinnamaldehyde with Pt And Pt-Fe catalysts: Effects of the support. *Braz. J. Chem. Eng.* **1998**, *15*, 140–144. [[CrossRef](#)]
39. Ananthan, S.A.; Narayanan, V. Liquid-phase hydrogenation of citral over Pt\_TiO<sub>2</sub> and Pt-Fe\_TiO<sub>2</sub> catalysts. *Asian J. Chem.* **2011**, *23*, 183–188.
40. Von Arx, M.; Mallat, T.; Baiker, A. Unprecedented selectivity behaviour in the hydrogenation of an  $\alpha,\beta$ -unsaturated ketone: Hydrogenation of ketoisophorone over alumina-supported Pt and Pd. *J. Mol. Catal. A Chem.* **1999**, *148*, 275–283. [[CrossRef](#)]
41. Fuente-Hernández, A.; Lee, R.; Béland, N.; Zamboni, I.; Lavoie, J.M. Reduction of Furfural to Furfuryl Alcohol in Liquid Phase over a Biochar-Supported Platinum Catalyst. *Energies* **2017**, *10*, 286. [[CrossRef](#)]
42. Chen, B.; Li, F.; Huang, Z.; Yuan, G. Tuning catalytic selectivity of liquid-phase hydrogenation of furfural via synergistic effects of supported bimetallic catalysts. *Appl. Catal. A Gen.* **2015**, *500*, 23–29. [[CrossRef](#)]
43. Shchukarev, A.; Korolkov, D. XPS study of group IA carbonates. *Open Chem.* **2004**, *2*, 347–362. [[CrossRef](#)]
44. Biesinger, M.C.; Payne, B.P.; Grosvenor, A.P.; Lau, L.W.; Gerson, A.R.; Smart, R.S.C. Resolving surface chemical states in XPS analysis of first row transition metals, oxides and hydroxides: Cr, Mn, Fe, Co and Ni. *Appl. Surf. Sci.* **2011**, *257*, 2717–2730. [[CrossRef](#)]